

Low- and High-Speed Flight Experiments on Transition Detection

I. Peltzer* and W. Nitsche†

Technische Universität Berlin, 10587 Berlin, Germany

and

J. Suttan‡

*MTU Maintenance Berlin-Brandenburg GmbH (Motoren- und Turbinen-Union),
14974 Ludwigsfelde, Germany*

DOI: 10.2514/1.35184

This paper describes in-flight measurements in low- and high-speed experiments to investigate laminar-turbulent transition on airfoils. The low-speed experiments were carried out using a laminar wing glove for a sailplane. High-speed experiments on an modified A320 hybrid laminar fin were conducted in close collaboration with Airbus. Different surface sensor measuring techniques (piezofoil, surface hot wires, wall microphones) were used in the low-speed experiments. The piezofoil technique was applied in the high-speed in-flight experiments to prove the operation robustness, the functional capability, durability, and reliability under atmospheric conditions in cruise flight on modern airplanes. All measuring techniques were successfully implemented for the particular task and the laminar-turbulent transition was detected with a high degree of certainty. For the high-speed investigations a complete piezofoil sensor array was glued directly to the fin without causing any interference between the boundary layer flow and the sensor foil. This technique therefore offered the good potential to detect transition in the boundary layer under flight conditions especially in high-speed tests.

Nomenclature

C	=	capacity
c	=	chord length
c_p	=	pressure distribution
d_T	=	pyroelectric coefficient
d_{33}	=	piezoelectric coefficient
E	=	voltage
f	=	frequency
OP	=	operational amplifier
R	=	resistance
Re_c	=	Reynolds number based on chord length
t	=	time
u_∞	=	freestream velocity
x	=	streamwise coordinate
z	=	spanwise coordinate
α	=	angle of attack
β	=	yaw angle for the vertical stabilizer
Δp	=	local, static pressure difference

I. Introduction

THE investigations presented in this paper are aimed at finding the laminar-turbulent transition in the boundary layer on an airfoil, particularly the spatial development and growth of flow instabilities such as Tollmien–Schlichting (TS) waves that lead to transition.

It is well known that the generation of TS waves strongly depends on the environmental flow conditions. It is therefore necessary to investigate the transition under real flight conditions as well as in

wind-tunnel tests. Based on the experience gained in the Deutsche Forschungsgemeinschaft-funded university group research project [1–3], where various measuring techniques for in-flight experiments were developed, this paper focuses mainly on measurements with polyvinylidene fluoride (PVDF)-sensor, surface hot wires as well as microphone sensor arrays and their feasibility to investigate and detect natural transition in flight experiments.

For industrial applications in the control of transition, for instance, a simple, robust and consistent measuring technique has to be developed and tested. This was only one reason for the A320 hybrid laminar fin (HLF) program, which was initialized by Airbus in the 1990s. The program was multinational as well as multidisciplinary including the extraordinary cooperation of industry, research establishments, universities and suppliers, as an essential part of the overall laminar flow research activities within Europe [4,5]. Besides the scientific interest in the understanding of flow physics including transition mechanisms, both technical and managerial objectives were involved. First of all, the A320 vertical tailplane fin was modified in a way to establish laminar flow over the fin box without modifying the box itself. Furthermore, a suction system was built into the fin nose to induce the hybrid laminar flow. Then measuring techniques based on experience gained in earlier wind-tunnel experiments were adapted for the A320 HLF. Among others, an infrared camera, a traversable wake rake, hot films, an array of PVDF sensors, temperature probes, and pressure taps were used to control and monitor the flight experiments [6].

The PVDF-sensor array, which could detect the laminar-turbulent transition on the fin, was applied by the Berlin Institute of Technology. Therefore, it could demonstrate the success of the suction system also. This paper will show the results of the high-speed tests with the PVDF-foil technique at the A320 HLF. These results will be compared with the results from the low-speed experiments on the Twin II laminar wing glove with respect to the potentials of the PVDF measuring technique.

II. Experimental Setup

A. Laminar Flow Wing Glove: G103

A laminar wing glove, which was developed for the Grob G103 Twin II two-seater sailplane at the Institute for Aeronautics and

Received 17 October 2007; accepted for publication 11 February 2008.
Copyright © 2008 by the American Institute of Aeronautics and Astronautics, Inc. All rights reserved. Copies of this paper may be made for personal or internal use, on condition that the copier pay the \$10.00 per-copy fee to the Copyright Clearance Center, Inc., 222 Rosewood Drive, Danvers, MA 01923; include the code 0021-8669/08 \$10.00 in correspondence with the CCC.

*Research Associate, Department of Aerodynamics, Institute of Aeronautics and Astronautics, Marchstrasse 12; inken.peltzer@tu-berlin.de.

†University Professor, Head of Department of Aerodynamics, Institute of Aeronautics and Astronautics, Marchstrasse 12.

‡Project Leader Restructuring SB, Dr.-Ernst-Zimmermann-Straße 2.



Fig. 1 Sailplane Grob G103 Twin II with the glove.

Astronautics, Berlin Institute of Technology, was used for the low-speed in-flight measurements (Fig. 1). The measuring glove has a 2-D center part with a 1.0 m span and a chord length of 1.22 m. It has an exchangeable wing segment that was equipped with different surface sensors or actuators. (One sensor setup is shown in Fig. 5.) An array of 69 PVDF sensors was used. A streamwise line of 17 sensors was located from 40 to 50% of the chord length to measure TS instabilities as a criterion for the different stages of transition. Four additional rows of 16 sensors each arranged in the spanwise direction were employed. The first spanwise piezosensor row was located at 46.3% and the fourth row at 49.6% of the chord length. There were 14 mm between each row and 7 mm between the spanwise sensors. Furthermore, surface hot wires and microphone sensor arrays were used on this glove. The flight experiments at the sailplane were mostly carried out at flight velocities from 22 to 30 m/s, resulting in a chord Reynolds number of $1.7 \times 10^6 < Re_c < 2.4 \times 10^6$.

The measurement system (Sec. III.A) is located in the equipment support underneath the glove. A Prandtl tube, which is also attached underneath the glove, is used to measure the freestream velocity. Because the angle of attack of a sailplane directly corresponds to the flight velocity by a defined wing loading, a certain flight velocity can describe the boundary conditions on the wing and on the glove, respectively. The differences in pressure between two pressure taps on the glove's top ($\Delta p_{x1,x2}$; $x_1/c = 37.2\%$, $x_2/c = 52\%$) are measured to get a second indication of the boundary conditions beside the freestream velocity. The pressure difference and the corresponding freestream velocity with a certain wing loading was measured in all flights. Figure 2 shows this correlation between the pressure difference (Δp) relating to the freestream velocity (u_∞) for some flights. A thermocouple and a manometer were used to measure the air temperature and the absolute atmospheric pressure. These parameters are continuously recorded to monitor the freestream boundary conditions. The flight tests were performed in very calm air in the mornings or in the late afternoons. The freestream turbulence level itself was not measured in these tests.

Most flight tests with the laminar wing glove were carried out at a freestream velocity of 23.6 m/s. For this velocity the sensor setups were applied on the glove. Figure 3 shows the velocity distribution of the glove's top side for in-flight measuring and a calculated velocity

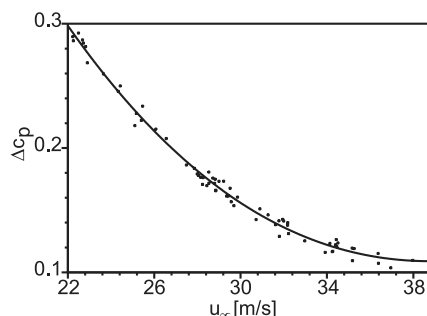


Fig. 2 Possible flight velocities with corresponding pressure differences on the glove.

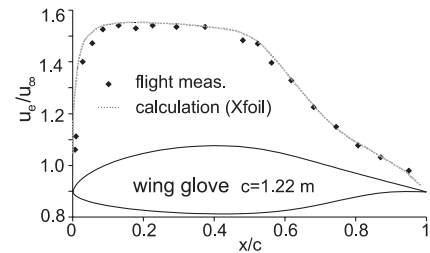


Fig. 3 Velocity distribution of the glove at $u_\infty = 23.6$ m/s.

distribution (Xfoil [7], $Re_c = 1.92 \times 10^6$, $\alpha = 5.4$ deg). By looking at Fig. 3, quite a good conformity between measurement and calculation can be observed. Furthermore, the glove flow shows a relatively long area with a weak increase of pressure and thus provides a moderate amplification of the unstable boundary layer disturbances. The amplification of the unstable disturbances was measured to describe the stages of transition on the glove.

B. Hybrid Laminar Flow Fin: A320

The in-flight experiments at higher Reynolds and Mach numbers were carried out on a modified A320 vertical tailplane (Fig. 4) in close collaboration with Airbus. A special PVDF-sensor array was built and attached to the upper part of the fin downstream of a suction panel, which was used to control the transition. The geometry of the PVDF array was defined through the position on the upper part of the fin. The array incorporated 32 sensors in two streamwise lines at a chord length of 23 to 52.6%. The distance between the equally spaced sensors was 1.97% of the chord length (≈ 56 mm) of the fin (Fig. 4). The complete sensor array was glued to the fin and was plugged into the borders. Interferences with the boundary layer flow through the sensor on the fin surface could not be observed.

Developing the sensor layout for this investigation, two streamwise sensor lines were produced to have fallback positions in case of sensor failure. All sensors were adjusted in ground tests to reach the same sensitivity and verified concerning their dynamic characteristics in the first flight tests. The best sensors were chosen for the interpretation of the measurements after this basic test (Fig. 4, active sensor). Generally the sensors had really similar characteristics and only a few of them failed.

The main objective of this part of the Berlin Institute of Technology within the scope of the A320 HLF program was to prove the functional capability, durability, and reliability of the PVDF-sensor technique under real atmospheric conditions in cruise flight. In particular, this means low temperatures (down to -60°) and high

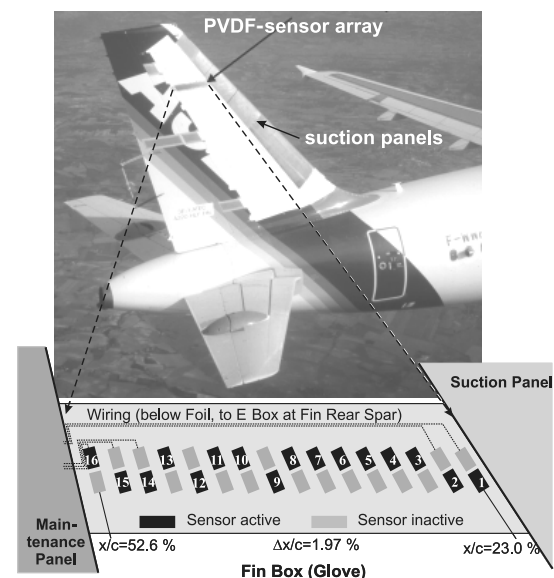


Fig. 4 A320 HLF fin and the PVDF-sensor array (photo: Airbus).

velocities (up to $Ma \approx 0.8$). Furthermore, the tests focused on the investigation of other environmental influences such as the noise level, resonance frequencies, or the acceleration occurring in modern airplanes. The established criterion to ensure transition detection is a sufficient signal-to-noise ratio (SNR, see also Sec. III.B).

In contrast to the measurements with the sailplane glove, where TS instabilities can be used to define the transition, the transition on the A320 fin is presumably initiated by cross-flow instabilities due to the sweep angle of the A320 tailplane [8–10]. The frequencies of instabilities in the high-speed case are higher than on the low-speed, two-dimensional glove on the sailplane. Therefore, the maxima of the rms values correspond to the intermittence and remain the criterion for transition in this case. The intermittence rate describes the probability of the occurrence of turbulent structures at a certain point in the flow. An intermittence of 50% can be considered the location of transition.

III. Sensor Techniques

A. Measurement Data Acquisition System

A miniaturized and modularly arranged measuring system especially developed for in-flight measurements was employed in both cases in order to record the data of the dense surface sensors at a high temporal resolution. This multichannel measurement data acquisition system (MEDAS) consists of two parts. One part of MEDAS (the electronic box) was located close to the sensor array at the rear spar of the fin or underneath the glove of the sailplane. The basics of this electronic box are a two-stage amplifier (charge and power amplifier for each channel) with electronically adjustable amplifier settings and a multiplexer, A/D converter, electric–optical converter next in line. The measuring computer in the cockpit includes the second, board part of MEDAS and makes it possible to control the measurement system on the fin and on the wing, respectively, during flight. Communication and data transfer for storage between both parts of the measurement system are carried out via fiber optical transmission. The sampling rate of each channel was about 30 kHz.

B. PVDF Sensor

PVDF-sensor arrays, well known as the piezofilm sensor technique, already have been successfully employed for measurements of unsteady surface force fluctuations on different applications for several years [11]. A PVDF-sensor array consists of a thin PVDF (polyvinylidenefluorid) film (10 to 100 μm thick), metallized on both sides (Fig. 5). The upper metallic side is used as an electric ground, thereby also serving as an electrostatic and electromagnetic shield. By partially etching one side of the metallic coating, it is possible to create sensor arrays which are customized for a given measurement task. Then each single sensor area is connected to the charge

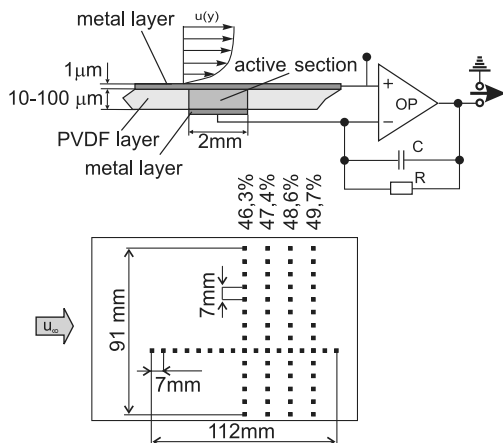


Fig. 5 Sketch of a single PVDF sensor and the PVDF-sensor array used for the laminar wing glove on GROB G103 Twin II.

amplifier via thin wires. A single PVDF sensor can be considered as a plate capacitor with very low capacity and mass. The PVDF material has both piezoelectric as well as pyroelectric properties.

When assuming a mechanical (piezoelectric) or a temperature (pyroelectric) change characteristic in laminar-turbulent transition, the sensor material produces small electric charges. The sensor signals can be amplified by means of simple charge amplifiers. The possible frequency range is limited only by the lower limiting frequency of the charge amplifier employed. The choice of the charge amplifier depends on the measuring task. Because the pyroelectric constant (which describes the pyroelectric properties) is some orders higher than the piezoelectric constant, a low-temperature gradient (<2 K) between sensor and fluid can be employed to obtain a higher SNR [12]. This can be important for the minimization of sensor size and spacing in array measurement techniques. Because of the closed foil on the wing surface, the sensor produces negligible roughness. In this case the experiments showed the successful production of large sensor arrays [areas up to $(1000 \times 220) \text{ mm}^2$] with a smooth and undisturbed surface. The cutoff frequency of the applied PVDF-sensor array (including the entire measuring system) was about 30 kHz; the sensor was therefore suitable for dynamic measurements at high velocities.

The custom-made sensor arrays used a 28 μm -thick polymer film (with a pyrocoefficient, $d_T = -30 \times 10^{-6} \text{ C/m}^2 \text{ K}$ and a piezocoefficient $d_{33} = -33 \times 10^{-12} \text{ C/N}$) sandwiched between two 1- μm Ni-Cu layers. In basic wind-tunnel experiments the upper one was coated using a 5- μm -thick TESATM film for protection from abrasive erosion. Both coated and noncoated sensors were tested. The results suggest that the coating layer has almost no effect at both low ($Ma = 0.3$) and high ($Ma = 0.5$) speeds [13]. Therefore, the coating can be used to protect the sensor surface in real applications.

C. Surface Hot-Wire Sensor

A principle sketch of the surface hot-wire sensor is shown in Fig. 6. A platinum-coated tungsten wire ($d = 5 \mu\text{m}$) is fixed over a narrow slot (0.075–0.1 mm) flush to the surface. For the sensor substrate, a flexible circuit board with a 30–75 μm copper layer is used. The slot can be easily shaped in the copper layer using the photoetching technique. This arrangement produces reduced heat flux in the structure. Therefore, a higher signal-to-noise ratio is achieved (compared to conventional hot-film sensor arrays) [14]. Modularly arranged hot-wire anemometers were designed especially for in-flight measurements to be able to operate a high number of surface hot-wire sensors during flight in constant-temperature mode. This highly sensitive wall sensor was developed especially for measuring the weakest wall shear stress fluctuations. Therefore, this sensor can be used for measuring the fluctuations and the amplification of the fluctuations in the boundary layer, where the maximum of amplification (determined as the maximum of the rms values) provides a criterion for the laminar-turbulent transition.

For this special task the laminar wing glove was equipped with a downstream row of surface hot-wire sensors. The spacing of the sensors is similar to the corresponding streamwise PVDF-sensor line mentioned previously (6.5 mm for the sailplane). The position of the first sensor was located farther downstream to measure the higher amplified stages of the TS waves and to observe the transition to turbulence. In this case the sensors were arranged between 45 and 55% of the chord. The surface hot-wire sensor shows the best

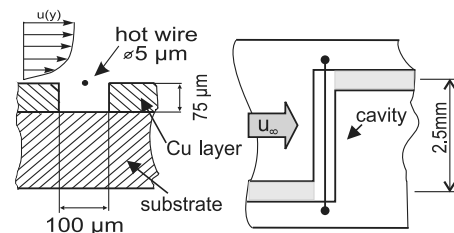


Fig. 6 Sketch of a single surface hot-wire sensor.

signal-to-noise ratio, but has a lower cut of frequency compared to pressure-sensitive measuring techniques (PVDF sensors). The distress from damage is especially high in high-speed flight tests, however.

D. Microphone Sensor

Another way of measuring TS waves and observing the laminar-turbulent transition is the installation of miniature microphones. Therefore, a microphone sensor array was installed on the exchangeable glove segment. Very small microphones were mounted underneath the surface with a 0.3 mm drilled hole. Figure 7 shows the principle sketch of the construction and the sensor positions. The microphones themselves have a sensitivity of -63 dB, a frequency range of 20–12,000 Hz and are 6.3 mm in diameter and 4.3 mm high. Because of this special construction the microphone array is probably of limited use for in-flight applications on large aircraft and high-speed measurements, but it supplies a sufficient database of the amplification of TS waves on the laminar wing of the sailplane.

All sensors were used as sensors to measure fluctuations in the boundary layer. Therefore, it was not essential to calibrate them to physically meaningful quantities. Sensors of a single array were adjusted with regard to each other. They have the same sensitivity within one setup. Generally, all sensors were suited to detecting transition. The PVDF sensor has some advantages in the high-speed case, especially for high frequencies and produces almost no roughness on the surface of the wing. It also has an active measuring principle, which requires less space for the implementation of the measurement equipment compared to the surface hot wire, which provides the best signal-to-noise ratio in a frequency range of up to 2 kHz. Microphone sensors are very simple to handle. The cutoff frequency depends on their installation (mounting height/position).

IV. Results

The process of laminar-turbulent transition on a basically two-dimensional airfoil can be described with three major aspects: receptivity, linear stability, and nonlinear breakdown [15]. The first aspect (receptivity) is devoted to the generation of instability waves (TS waves) in the region of the airfoil's leading edge, where instability waves are amplified. This aspect is not considered in this paper. The second stage of transition (linear stability) corresponds to the development and amplification of instabilities. This stage shows characteristic structures within the boundary layer. Surface sensor arrays can measure these structures by means of the so-called "footprint" of the boundary layer, too. The following sections show the amplification of the instabilities in time traces of streamwise-located sensors of such a footprint. The third stage (nonlinear breakdown) is specified by means of the rms values of the streamwise sensor signals. The rms values at the first stage are very low and are subsequently increased with the amplification of the instability. The maximum of rms values characterizes the transition (nonlinear breakdown) that is almost finished. Then the rms values decrease to a lower level that is higher than in the laminar boundary layer. This represents the turbulent stage.

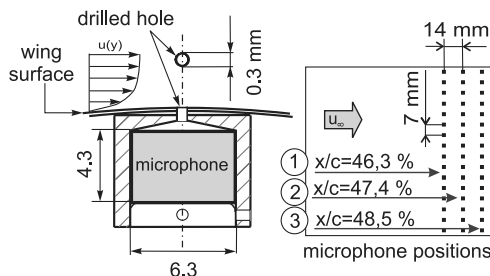


Fig. 7 Sketch of installation and positions of the miniature microphones.

A. Laminar-Turbulent Transition in Low-Speed Flight Tests

1. PVDF-Sensor Arrays

At first, results of the in-flight measurements with the sailplane are discussed. These experiments were carried out at velocities ranging from 22 to 30 m/s as mentioned above. The sensor array employed had a streamwise line of PVDF sensors of 30 to 55% chord length. This array could detect the transition in the range of freestream velocity mentioned. The rms values at different velocities of the streamwise sensor line are shown in Fig. 8. Each graph has a maximum that indicates the laminar-turbulent transition. The maximum shifts downstream with increasing velocity, because an increasing velocity corresponds with a decreasing angle of attack of a sailplane. Therefore, with increasing velocity the transition moves downstream, as can be seen in this figure. Furthermore, the rms values are on the same low level up to a chord length of 35%. The increase of rms values starts at a later chord with respect to the increasing velocity. Because the stability of the boundary layer depends on the pressure gradient, the amplification of instabilities is related to the angle of attack. Because of the change in stability at different velocities, the amplification does not only start later but also more quickly (steeper) and with a higher level of the maximum rms value. The range from amplification of TS instabilities to the turbulent breakdown is smaller at higher velocities and at lower angles of attack, respectively. After reaching the maximum, the rms values decrease again for the turbulent boundary layer.

Figure 9 shows the significant raw and filtered time traces over 50 ms of streamwise PVDF sensors on the wing glove. The PVDF-sensor array employed contains 17 streamwise sensors of ≈ 40 to $\approx 50\%$ chord length and is shown in Fig. 5. The signals were measured at a flight velocity of 23.6 m/s. Figure 9a shows the raw data of the PVDF sensors. Up to the eighth sensor the signals are very smooth and no characteristic disturbances or instability waves can be identified. Subsequently, wave packets occur with the amplitude increasing with the chord length. Furthermore, the temporal phase shift from one sensor to the next becomes apparent, which shows the convective transport process of the instability waves.

Figure 9b shows data of the same measurement; the signals are a filtered bandpass in the range of 200–1800 Hz, however. Up to a chord of around 47% the signals are very smooth again; through the bandpass filter the characteristic disturbances (wave packets) with very low amplitudes can be seen. Also, the temporal phase shift is more clearly seen. As can be seen so far, the PVDF-sensor technique is suitable for detecting the transition in low-speed in-flight experiments.

2. Surface Hot-Wire Sensor Array

With a view to the surface hot-wire sensor technique, significant time traces exceeding 60 ms of the streamwise arranged sensors (from ≈ 45 to $\approx 55\%$) are shown in Fig. 10. These signals are raw signals at two different flight velocities. Obviously, these signals illustrate the typical TS-wave packets without any filter. From the early beginning amplification stage the instabilities can be observed. Only a few electrical disturbances occur in the signals, which could

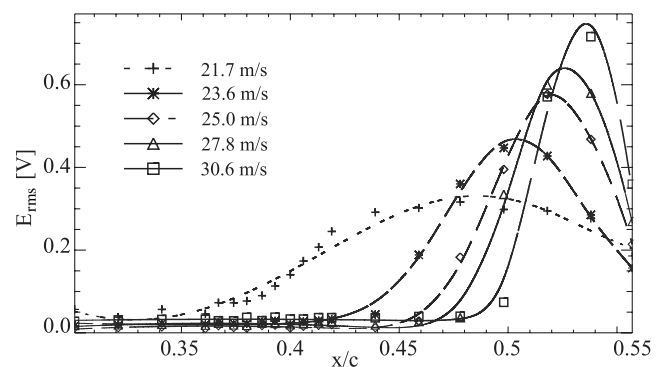
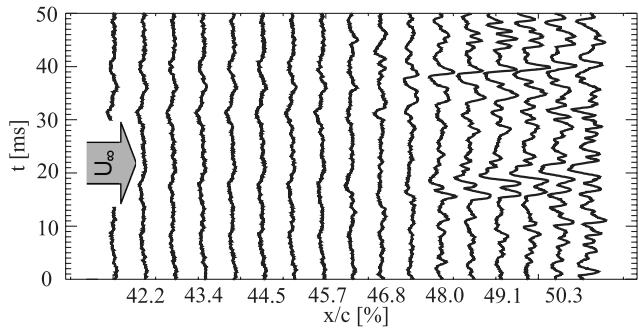
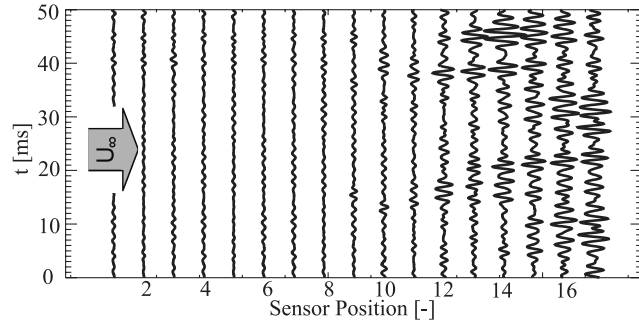


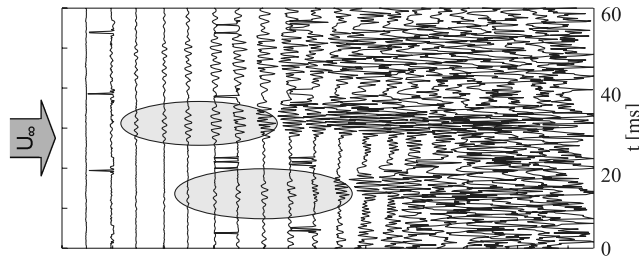
Fig. 8 RMS values of the streamwise PVDF sensors on the wing glove [18].



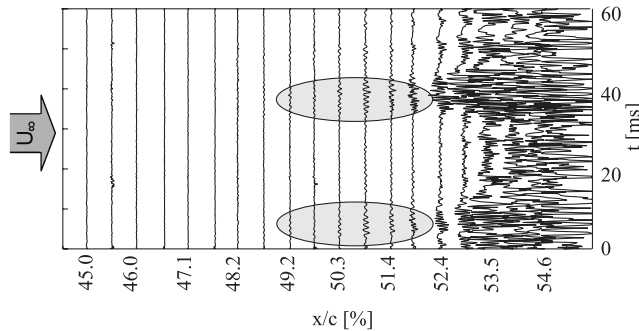
a)



b)

Fig. 9 a) Raw and b) filtered signals of the streamwise PVDF-sensor line at $u_\infty = 23.6$ m/s.


a)



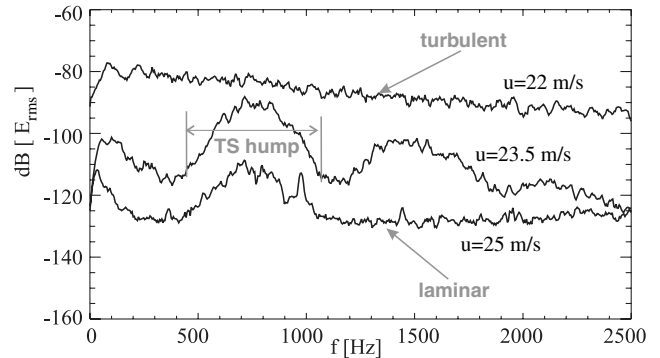
b)

Fig. 10 Raw signals of the streamwise arranged surface hot-wire sensors a) $u_\infty = 22.2$ m/s and b) $u_\infty = 27.8$ m/s

be easily eliminated through a signal conditioner and which do not falsify the flow information.

Furthermore, the spectral analysis of the signals allows some more conclusions from the predominant stage of the boundary layer. By looking at the frequency spectrum of one single surface hot wire of a chord length of about 50% at three different flight velocities, three different amplification stages can be registered.

Figure 11 shows three such frequency spectra. The lowest spectrum shows the frequency band selective amplification of the instable frequencies of about 500 to 1000 Hz (the so-called TS hump). This frequency band rises till it reaches saturation. At this


Fig. 11 Frequency spectra of a surface hot-wire sensor at a 50% chord length at three different flight velocities.

stage of the boundary layer, the higher harmonic frequencies were also amplified, as can be seen in the spectrum above the lowest one. All frequencies with higher amplitudes are represented, yet the fundamental frequency range clearly rises from the spectrum. There are also two more increased ranges. A frequency band limited amplitude increase can be found in the range of 1200–1800 Hz and a weaker one is apparent in the range from 2000–2300 Hz. These ranges reflect the amplification of the first and second higher harmonic frequencies, that is, the boundary layer is already at a nonlinear amplification stage here. In the third spectrum, the amplification of all frequencies is increased so much that the TS hump no longer stands out of the spectrum, that is, the boundary layer is predominantly turbulent.

3. Microphone Sensor Array

Next, results obtained from in-flight measurements employing the microphone sensor array are discussed. Figure 12 illustrates filtered time traces from the three spanwise microphone sensor rows at a flight velocity of $u_\infty = 23.6$ m/s. For a start, the time traces of the first row show typical TS instabilities with a relatively small amplitude. No temporal phase shifts between adjacent sensors can be observed, and so the instabilities propagated are still two dimensional. In the next chart (Fig. 12b), the time traces of the second row show increased signal amplitudes. In addition to the increased amplitudes, the third row (Fig. 12c) illustrates the amplification of frequencies which are not the fundamental TS-frequency range. The contour plot (Fig. 13) of 15 ms of the time traces of the third row indicates a temporal phase shift in the spanwise adjacent sensors. This temporal phase shift suggests the development of three-dimensional instability structures and the beginning of a nonlinear transition stage.

This is confirmed by the varying amplified signal amplitudes of the spanwise adjacent sensors in the third row, in contrast to the uniform amplified instabilities in the first row. As mentioned previously, the early linear stage of transition is characterized through the spanwise, two-dimensional amplification of instability waves.

The middle chart of Fig. 14 shows the frequency spectrum of the fourth sensor (highlighted in Fig. 12) of each row. Looking at the highest frequency spectrum (Fig. 14b), the fundamental TS hump still dominates the spectrum with the first and second harmonic frequencies increasing as well. The spectra of the microphones on the first and second row show similar characteristics at a lower level. Specifically, on the first row at 46.3% of the chord only the first higher harmonic frequencies occur. The increase in the fundamental frequencies from the second to the third row is minimal. Therefore, the higher harmonic frequencies increase significantly.

Caused by a lower flight velocity (a different pressure distribution, respectively) (Fig. 14c) all spectra are on a higher level, so that the higher harmonic frequencies almost disappear in the spectra. The transition has proceeded farther than at a higher velocity. In the case of a velocity of 25 m/s only the fundamental frequencies are amplified (Fig. 14a). Altogether the spectra in this case are on the lowest level, compared to all other spectra shown. The transition is at

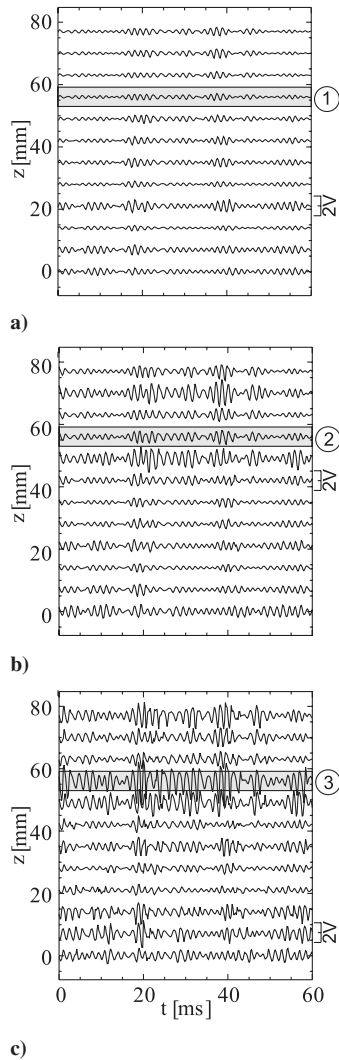


Fig. 12 Filtered time traces of microphone sensors at a velocity of 23.6 m/s, a) row 1, $x/c = 46.3\%$; b) row 2, $x/c = 47.4\%$; and c) row 3, $x/c = 48.5\%$.

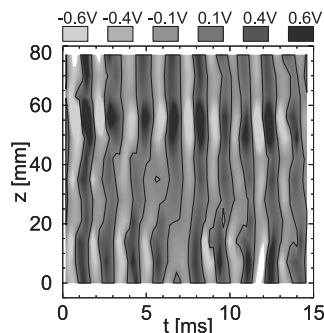


Fig. 13 Contour plot of 15 ms of the time traces of the spanwise microphone sensors, row 3, $x/c = 48.5\%$, $u_\infty = 23.6$ m/s.

an early, linear stage. These results clearly correspond to the measurements with surface hot wires (Fig. 11, at 50% chord length).

B. Laminar-Turbulent Transition in High-Speed Flight Tests

The results of the measurements using PVDF-sensor arrays in high-speed flight tests are given later. The tests were performed at Mach numbers of up to 0.8 that correspond to flow velocities of up to 330 kt and at altitudes of about 11,000 m. Figure 15 shows an example of significant time traces over 800 ms of the streamwise PVDF sensors (the overall time trace length was 6.5 s). On the first

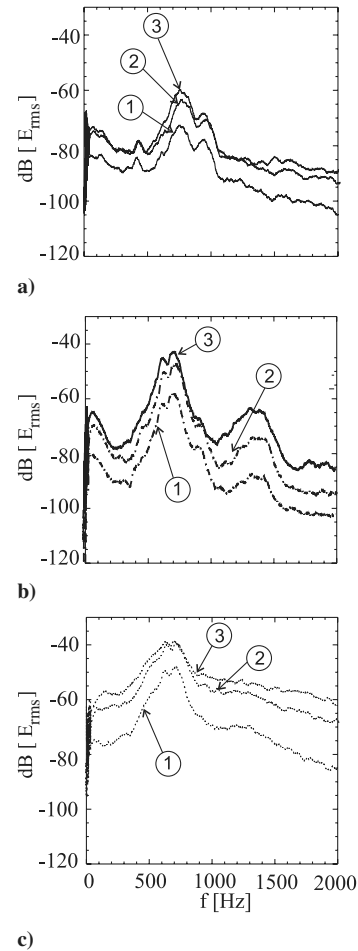


Fig. 14 Spectra of one microphone sensor per row at three flight velocities, a) 25 m/s; b) 23.6 m/s; and c) 22.2 m/s.

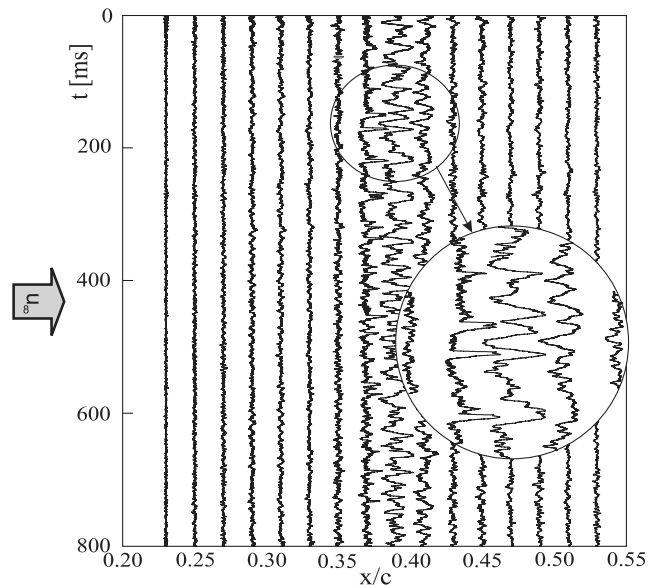


Fig. 15 Time traces of the PVDF sensors on the A320 HLF.

sensor in the streamwise direction the signal is smooth and shows no amplification of instability waves at all. On the next sensors a small amplification can be observed (linear stage). At a chord length of $x/c = 0.37$ the amplitudes of the sensors are increasingly stronger. Transitional structures, such as “spikes” or “turbulent spots,” occur (nonlinear stage). The high amplitudes of the signal at 0.39% of the chord represent the last stage of laminar-turbulent transition. At a

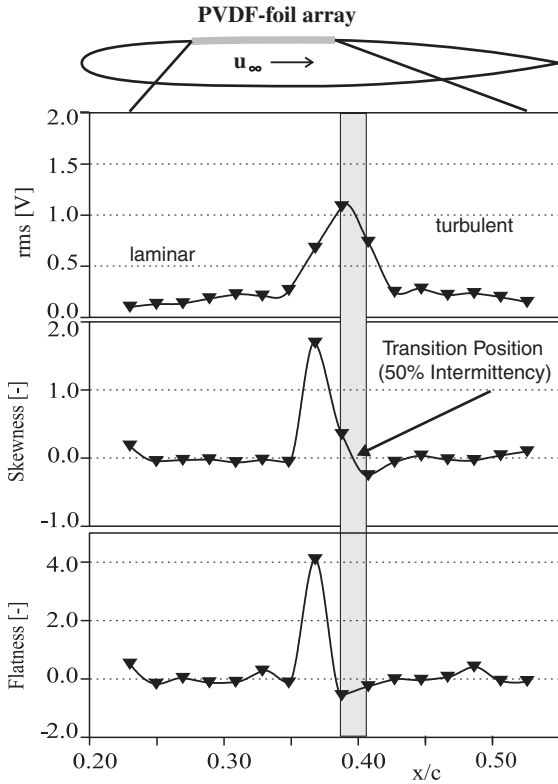


Fig. 16 Transition detection on the fin with rms values, skewness, and flatness.

chord length of 0.41 the amplitudes are decreased, meaning the boundary layer flow is turbulent. The signals are bandpass filtered. Therefore, the structures in the turbulent boundary layer are not included in the signals after filtering.

The averaged data and the results of the statistical data analysis are shown in Fig. 16. Analogous to the analysis of the in-flight measurements on the sailplane, the rms values of the 16 streamwise arranged PVDF sensors for one single measuring point are shown in the first chart of this figure. The rms values start at a very low level and subsequently increase because of the amplification of instabilities. They reach a maximum and decrease to a lower level. Therefore, they indicate the transition location. Because the rms values are also calculated from the bandpass filtered signals, their level at the laminar stage is about the same as at the turbulent stage of transition. They determine high amplitudes of the fluctuations, with respect to intermittence and the occurrence of turbulent structures at a certain point.

Further statistical analyses were performed by means of skewness and flatness [16]. The skewness describes the asymmetry of the distribution of the amplitudes based on a Gauss distribution. In the laminar boundary layer the skewness is close to zero and reaches its maximum at the late stage of transition (25% intermittence). At transition (50% intermittence) the skewness has zero crossing. The flatness describes the width of the amplitude distribution and can be considered as a rate of the power dispersion of the system. Therefore, the maximum of the rms values together with skewness and flatness is sufficient criteria for transition detection. A similar signal performance was observed at almost all other measuring points. Further experiments investigated the influence of the yaw angle of the tailplane (vertical stabilizer), which means the pitch of a profile and the suction rate. Figure 17 shows the results of one test case of this variation based on the rms values of the streamwise PVDF sensors. Clearly, the influence of the yaw angle on the transition is much higher than a variation of the suction. Although the suction variation shifts the transition by about 2%, a different yaw angle can cause a transition shift in the range of 15% of the chord length. That was to be expected because the transition depends on the pressure distribution. The pressure distributions in turn change significantly

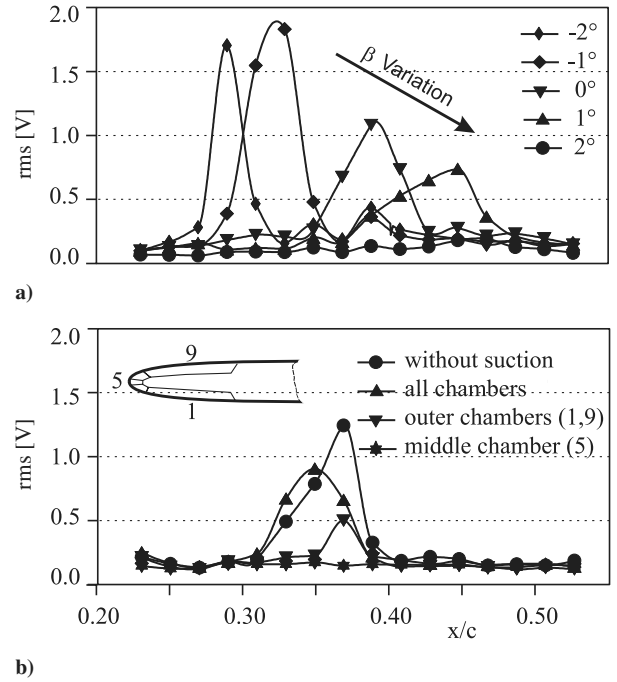


Fig. 17 Influence of the yaw angle and the suction rate on transition.

with changing yaw angles; consequently, the boundary layer has different stability properties at different yaw angles. Therefore, not only the position of the maximum rms value changes, but the maximum amplitude itself can vary, too. These completed high-speed flight experiments proved the reliability of the PVDF-sensor technique under operational conditions in cruise flight, which was the task assigned to the Berlin Institute of Technology within the A320 HLF program.

V. Conclusions

This paper reports a successful low- and high-speed transition-detection measuring technique on laminar airfoils. Low-speed in-flight experiments were carried out on a sailplane using a laminar wing glove. High-speed experiments were conducted on the A320 hybrid laminar fin in close collaboration with Airbus. On the laminar wing glove different surface-sensor techniques (surface hot-wire arrays, microphone arrays, and PVDF-foil sensor arrays) were employed. These low-speed experiments clearly show Tollmien-Schlichting instabilities at an early stage of growth, and also the amplification of these instabilities, the convective character of the transition mechanisms, and finally the breakdown to turbulent structures in the boundary layer. In contrast to the pressure-sensitive measuring techniques (piezofoil), the surface hot-wire sensor shows a decreasing sensitivity with increasing speed (low-speed experiments), but the best signal-to-noise ratio in low-speed experiments. Although, this proves all applied measuring techniques are suitable for detecting transition by measuring the surface force fluctuations in the laminar boundary layer on the wing surface.

Subsequently the PVDF-foil technique was applied in high-speed in-flight experiments to additionally prove the operational robustness and the functional capability in cruise flight of modern airplanes. The results obtained from these experiments show the amplification of instabilities (i.e., turbulent spots) as well as the transition to turbulence in the boundary layer. The cutoff frequency of the applied PVDF-sensor system was about 30 kHz, proving the sensor to be highly suitable for dynamic measurements also at high Mach numbers. Furthermore, the investigations show the potential of the PVDF-foil measuring technique under atmospheric conditions to detect, for instance, transition or shock phenomena [17] in the boundary layer. In addition, this sensor does not disturb the surface of the wing and the space required for the electronic equipment is minimal.

Acknowledgments

The financial support of the research project by the government within the Luftfahrtforschungs- und Technologieprogramm of the Federal Republic of Germany (reference FKZ 20A9801) and of the research project by the DFG (German Research Foundation, reference Ni 282/12) is gratefully acknowledged. Special thanks go to Airbus, where the in-flight measurements on the A320 fin were conducted.

References

- [1] Nitsche, W., Suttan, J., Becker, S., Erb, P., Kloker, M., and Stemmer, C., "Experimental and Numerical Investigations of Controlled Transition in Low-Speed Free Flight," *Aerospace Science and Technology*, Vol. 5, No. 4, 2001, pp. 245–255.
doi:10.1016/S1270-9638(01)01105-1
- [2] Seitz, A., "Evaluation of Initial Amplitudes of Free-Stream Excited Tollmien-Schlichting Waves from Flight-Test Data," *New Results in Numerical and Experimental Fluid Mechanics VI*, edited by C. Tropea, S. Jakirlic, H.-J. Heinemann, R. Henke, and H. Hönliger, Vol. 96, Notes on Numerical Fluid Mechanics and Multidisciplinary Design, Springer-Verlag, Berlin, 2008, pp. 260–267.
doi:10.1007/978-3-540-74460-3_32
- [3] Hausmann, F., and Schröder, W., "Coated Hot-Film Sensors for Transition Detection in Cruise Flight," *Journal of Aircraft*, Vol. 43, No. 2, 2006, pp. 456–465.
doi:10.2514/1.14825
- [4] Henke, R., "Airbus A320 HLF Fin Flight Tests," *Aerodynamic Drag Reduction Technologies*, edited by P. Thiede, Vol. 76, Notes on Numerical Fluid Mechanics, Springer-Verlag, Berlin, 2001, pp. 31–36.
- [5] Thibert, J., Quast, A., and Robert, J., "The A320 Laminar Fin Programme," *Proceedings—First European Forum on Laminar Flow Technology, Hamburg*, DLGR-Bericht 92-06, Deutsche Gesellschaft für Luft- und Raumfahrt, Bonn, Germany, 1992, pp. 19–25.
- [6] Kühn, W., Strahmann, J., Höhler, G., and Quast, A., "Measuring Techniques for A320 Fin Reference and Hybrid Laminar Flight Tests," *2nd European Forum on Laminar Flow Technology, Bordeaux*, Confederation of European Aerospace Societies, Association Aéronautique et Astronautique de France, Paris, France, 1996, pp. 7.16–7.28.
- [7] Drela, M., *Xfoil—User Guide*, 6th ed., MIT Aero&Astro Harold Youngren, Dec. 2001, <http://raphael.mit.edu/xfoil>.
- [8] Janke, E., Bertolotti, F., Hein, S., Koch, W., Stolte, A., Theofilis, V., and Dallmann, U., "Receptivity Processes and Transition Scenarios for Swept-Wing Flows with HLF Technology," *Aerodynamic Drag Reduction Technologies*, edited by P. Thiede, Vol. 76, Notes on Numerical Fluid Mechanics, Springer-Verlag, Berlin, 2001, pp. 172–179.
- [9] Abegg, C., Bippes, H., Boiko, A., Krishnan, V., Lerche, T., Pöthke, A., Wu, Y., and Dallmann, U., "Transitional Flow Physics and Flow Control for Swept Wings: Experiments on Boundary-Layer Receptivity, Instability Excitation and HLF Technology," *Aerodynamic Drag Reduction Technologies*, edited by P. Thiede, Vol. 76, Notes on Numerical Fluid Mechanics, Springer-Verlag, Berlin, 2001, pp. 199–206.
- [10] Schrauf, G., "Large-Scale Laminar-Flow Tests Evaluated with Linear Stability Theory," *Journal of Aircraft*, Vol. 41, No. 2, 2004, pp. 224–230.
doi:10.2514/1.9280
- [11] Nitsche, W., Mirow, P., and Szodruch, J., "Piezo-Electric Foils as a Means of Sensing Unsteady Surface Forces," *Experiments in Fluids*, Vol. 7, No. 2, 1989, pp. 111–118.
doi:10.1007/BF00207303
- [12] Sturzebecher, D., and Nitsche, W., "Visualization of the Spatial-Temporal Instability Wave Development in a Laminar Boundary Layer by Means of a Heated PVDF Sensor Array," *New Results in Numerical and Experimental Fluid Mechanics*, edited by H. Körner, and R. Hilbig, Vol. 60, Notes on Numerical Fluid Mechanics, Vieweg Verlag, Braunschweig, 1997, pp. 335–342.
- [13] Burkardt, O., Dinata, U., and Nitsche, W., "Surface Fence with an Integrated, Piezoresistive Pressure Sensor for Measurements of Static and Dynamic Wall Shear Stress," *New Results in Numerical and Experimental Fluid Mechanics III*, edited by S. Wagner, U. Rist, J. Heinemann, and R. Hilbig, Vol. 77, Notes on Numerical Fluid Mechanics, Springer-Verlag, Berlin, 2002, pp. 411–418.
- [14] Sturzebecher, D., Anders, S., and Nitsche, W., "The Surface Hot Wire as a Means of Measuring Mean and Fluctuating Wall Shear Stresses," *Experiments in Fluids*, Vol. 31, No. 3, 2001, pp. 294–301.
doi:10.1007/s003480100284
- [15] Kachanov, Y., "Physical Mechanisms of Boundary-Layer Transition," *Annual Review of Fluid Mechanics*, Vol. 26, Jan. 1994, pp. 411–482.
10.1146/annurev.fl.26.010194.002211.
- [16] Siddall, J. N., *Probabilistic Engineering Design*, Vol. 23, Mechanical Engineering, Marcel Dekker, New York, 1983, 1st ed.
- [17] Nitsche, W., Swoboda, M., and Mirow, P., "Shock Detection by Means of Piezofoil," *Zeitschrift für Flugwissenschaft und Weltraumforschung*, Vol. 15, Aug. 1991, pp. 223–226.
- [18] Peltzer, I., and Nitsche, W., "In-Flight and Wind Tunnel Measurements of Natural and of Controlled Instabilities on a Laminar Flow Airfoil," *Sixth IUTAM Symposium on Laminar-Turbulent Transition*, edited by R. Govindarajan, Vol. 78, Fluid Mechanics and its Applications, Springer-Verlag, The Netherlands, 2006, pp. 261–266.
10.1007/1-4020-4159-4_35.